Surfactant-Free Cellulose Filaments Stabilized Oil in Water Emulsions

Amir Varamesh
University of Calgary
Ragesh Prathapan
University of Calgary
Ali Telmadarreie
University of Calgary
Jia Li
University of Calgary
Keith Gourlay
Performance BioFilaments
Gurminder Minhas
Performance BioFilaments
Qingye Lu
University of Calgary
Steven L. Bryant
University of Calgary
Jinguang Hu (jinguang.hu@ucalgary.ca)
University of Calgary Schulich School of Engineering https://orcid.org/0000-0001-8033-7102

Research Article

Keywords: Pickering emulsions, cellulose filaments, carbohydrate binding module, green materials, oil in water emulsions, nano/microfibrillated cellulose

Posted Date: April 19th, 2021

DOI: https://doi.org/10.21203/rs.3.rs-374430/v1

Version of Record: A version of this preprint was published at Cellulose on December 2nd, 2021. See the published version at https://doi.org/10.1007/s10570-021-04320-9.

Surfactant-Free Cellulose Filaments Stabilized Oil in Water Emulsions

Amir Varamesh[1], Ragesh Prathapan[1], Ali Telmadarreie[1], Jia Li[1], Keith Gourlay[2], Gurminder Minhas[2], Qingye Lu[1], Steven L. Bryant[1,*], Jinguang Hu[1,*]

1. Department of Chemical and Petroleum Engineering, University of Calgary, Calgary T2N 1N4, Canada

2. Performance BioFilaments, 700 West Pender Street, Vancouver V6C 1G8, Canada

***Abstract:** There has been significant interest over recent years in the production and application of sustainable and green materials. Among these, nanocellulose has incurred great interest because of its exceptional properties and wide range of potential applications, including in Pickering emulsions. However, the production cost of these cellulosic materials has limited their application. In this study, the capability of a new type of cheaper cellulosic material, cellulose filaments (CFs), in formulating stable oil in water Pickering emulsions was investigated and compared with three conventional nanocelluloses, namely cellulose nanocrystals (CNCs), cellulose nanofibrils (CNFs) and TEMPO-oxidized CNFs (TEMPO-CNFs). Results showed that CFs can provide stable surfactant-free emulsions over wide ranges of salt concentration (0 – 500 mM) and pH (2 – 10), as indicated by the near constant oil droplet size and dewatering index of the emulsions. This is due to the ability of CFs to strongly adsorb to the oil and water interface, as evidenced by visualizing labeled CFs with engineered carbohydrate-binding module (CBM2a) conjugated with green

* Corresponding authors: Steven L. Bryant (steven.bryant@ucalgary.ca), Jinguang Hu (jinguang.hu@ucalgary.ca)

fluorescent protein (CBM2a-eGFP) under fluorescent microscopy. Compared to the emulsions stabilized by other types of nanocelluloses, the CFs-stabilized emulsion demonstrated a larger average droplet size and comparable (with CNFs) or better (than CNCs and TEMPO-CNFs) stability, which is partially attributed to the higher viscosity of continuous phase in the presence of CFs. The results of this study demonstrate the use of CFs as a novel and cheaper cellulosic material for stabilizing emulsions, which opens the door to a range of markets from the food industry to engineering applications.

Keywords: Pickering emulsions; cellulose filaments; carbohydrate binding module; green materials; oil in water emulsions; nano/microfibrillated cellulose

1. Introduction

Emulsions are colloidal systems in which droplets of a liquid phase are dispersed in another liquid phase (Schramm 2014). Generally, one of the liquid phases is aqueous while the other one is the hydrocarbon or oil phase. Depending on the dispersed and continuous phase, emulsions are primarily categorized into oil in water and water in oil wherein water forms the continuous and dispersed phase respectively (Schramm 2014). Emulsions are widely applicable in a plethora of industries, including food (Shao et al. 2020), membranes (Ahmad et al. 2019), drug delivery (Yan et al. 2019), cosmetic (Venkataramani et al. 2020), personal care (Marto et al. 2018), pharmaceutical (Kiss et al. 2011), energy storage (Zhang et al. 2019), and oil and gas (Zhou et al. 2019), and their stability is of high significance.

Emulsions have a free energy of formation of greater than zero, making them fundamentally thermodynamically unstable with a tendency to destabilize (Ghosh 2009). Thus, stabilizers or

emulsifiers are often used to form stable emulsions. Soluble surfactants and polymers are two conventional surface-active stabilizers that have been used for making stable emulsions (Jiang et al. 2020). However, conventional emulsions that are stabilized by either surfactants or polymers tend to show poor stability when exposed to change in pH, temperature or ionic strength. Moreover, some surfactants are toxic, have negative environmental footprints and can have adverse effects on health. Additionally, it has been demonstrated that the usage of surfactants and polymers can be prohibitively expensive for some processes (Khan et al. 2018; Gonzalez Ortiz et al. 2020; Shi et al. 2020).

Another interesting way of formulating stable emulsion is via the incorporation of solid particles as replacements for conventional surface-active materials. These types of emulsions are called Pickering emulsions, based on pioneering work by Ramsden and Pickering in the early 20th century (Ramsden 1904; Pickering 1907). Pickering emulsions are beneficial in comparison to traditional emulsions because of their superior stability against creaming, sedimentation, coalescence and flocculation (Shi et al. 2020; Zhang et al. 2020). During the emulsification process, particles are partially wetted by both liquid phases, reducing the interfacial free energy between them and enabling the formation of a packed layer at the interface of the liquids (Shi et al. 2020; Yan et al. 2020). Additionally, solid particles can also form a strong network in the continuous phase, preventing the merging of the droplets while enhancing the viscosity and further stabilizing the emulsions (Low et al. 2020; Shi et al. 2020; Yan et al. 2020).

The wettability of the particles, which is demonstrated by the three-phase contact angle at the interface, is a crucial factor regarding the formation of Pickering emulsions (Ragesh et al. 2014; Wu et al. 2020). Besides wettability, several other factors including pH of the continuous phase, ionic strength, and the concentration and shape of the particles control the emulsification process

and emulsion stability (Li et al. 2018; Mikulcová et al. 2018; Varanasi et al. 2018; Zhao et al. 2019).

Previously, several types of solid particles have been applied as stabilizers for Pickering emulsions, including (i) inorganic particles such as silica (Xue et al. 2017; Björkegren et al. 2020), metal oxide particles (Xie et al. 2017; Fessi et al. 2019), graphene (He et al. 2013), calcium carbonate (Zhu et al. 2013), etc.; (ii) polymeric particles such as polystyrene (Jiang et al. 2019; Li et al. 2019); and (iii) food-grade particles such as starch (Zhu 2019), chitin (Jiménez-Saelices et al. 2020), whey (Lee et al. 2020), etc.

With the growing demand for sustainable materials with reduced environmental footprints and with green and energy-efficient production routes, the application of natural materials has attracted increasing attention. Among such materials, nanocellulose (e.g. cellulose nanocrystals (CNCs), cellulose nanofibrils (CNFs), and TEMPO-oxidized CNFs) have received significant interest due to their sustainability, renewability, nontoxicity, biodegradability, and biocompatibility (Prathapan et al. 2016). For example, Pandey et al (Pandey et al. 2018a, b) investigated the ability of two different CNCs with various degrees of surface charge in stabilizing oil in water emulsions, and found that CNCs with lower surface charge have faster adsorption kinetic and formulate emulsions with smaller droplet size. Bai et al (Bai et al. 2019) employed high-energy microfluidization to stabilize oil in water emulsions using CNCs, which showed good stability over NaCl range of lower than 100 mm and pH range of 3 – 10. Aaen et al. (Aaen et al. 2019) demonstrated that both enzymatically treated CNFs and TEMPO-oxidized CNFs can result in stable rapeseed oil in water emulsions. Their results showed that enzymatically treated CNFs can be stable in the presence of NaCl and at low pH with only a slight increase in droplet size, while TEMPO-oxidized CNFs are unstable at these harsh conditions.

As described above, there are several studies available in the literature on the application of different types of nanocellulose on stabilizing Picketing emulsions. However, these nanocelluloses are expensive and there is still strong demand to produce cheaper and more effective cellulose-based materials for formulating Pickering emulsions. Cellulose filaments (CFs) are an emerging class of "nanocellulose", which contains a heterogeneous combination of fine and long nano/microfibrillar materials and are produced using a relatively cheap production process. CFs can be manufactured from a variety of bleached or unbleached wood pulps using simple mechanical shearing and without chemical or enzymatic treatments (Hamad et al. 2019; D'Acierno et al. 2020). The application of CFs has been explored in many fields but limited information is available for stabilizing Pickering emulsions. Herein, this study aims to investigate the formulation and characterization of oil-water Pickering emulsions stabilized by commercially available CFs. The effect of particle concentration and environmental stresses including ionic strength and pH on the stability of the emulsion are evaluated. The emulsifying ability of the CFs is compared to other types of nanocelluloses including CNF, CNC and TEMPO-oxidized CNF. The characterization of the emulsions was performed by dynamic light scattering, zeta potential measurements, optical microscopy, viscosity measurements, and fluorescent microscopy.

2. Materials and Methods

2.1. Materials

Cellulose filaments (CFs) at 10.0 wt% consistency was kindly given by Performance BioFilaments, BC, Canada. Cellulose nanocrystals (CNCs), cellulose nanofibrils (CNFs) and TEMPO-oxidized cellulose nanofibrils (TEMPO-CNFs) were obtained from CelluForce and Cellulose Lab, Canada. All the celluloses were used as supplied without any further modification. Water was purified by

the Mili-Q water purification system. Dodecane (anhydrous > 99%) were purchased from Sigma Aldrich, Canada, and were used as received for the oil phase. Oil Blue N (Dye content 96%. Sigma Aldrich) was used to label the dodecane. Enhanced green fluorescent protein fused carbohydrate-binding module 2a (CBM2a-eGFP) was synthesized in-house as described in the literature and used for fluorescent labelling of the CFs (Hu et al. 2014; Gourlay et al. 2015). Sodium chloride (NaCl), hydrochloric acid (HCl) and sodium hydroxide (NaOH) were obtained from Sigma Aldrich, Canada.

2.2. Preparation and Characterization of the Cellulose Suspensions

2.2.1. Preparation of cellulose suspensions

Cellulose suspensions were prepared by adding an appropriate amount of celluloses in water, which is then sonicated for 10 minutes (Branson 2800 series). The sample is then ultrasonicated in an ice bath (Qsonica Q700 sonicator) with 50% of maximum amplitude with 1 minute on and 30 seconds off interval to receive an energy input of 10 KJ for a 20 cc sample. The pH of the suspensions was adjusted by using HCl and NaOH solutions whereas NaCl was added to modify the salt concentration.

2.2.2. Dynamic light scattering, ζ-potential and Scanning Electron Microscopy

The apparent hydrodynamic diameter and ζ-potential of the cellulose samples were measured using a Particulate Systems Nano Plus HD nanoparticle/zeta analyzer. Dynamic light scattering (DLS) measurements were performed on suspensions with 0.1 wt% cellulose concentration and measurements were repeated 15 times to obtain an average value. ζ-potential measurements were done on cellulose dispersions with 0.025 wt% concentration and measurements were repeated at least 5 times.

Scanning electron microscopy (SEM) was conducted using a Hitachi S 300 N system (Tokyo, Japan). CFs sample with 0.5 wt% concentration was freeze-dried to perform SEM observations. Before imaging, to build up charge on the surface, the sample was coted with Pd-Au alloy.

2.2.3. Viscosity measurements

For measuring the viscosity of 0.5 and 1.0 wt% CF suspensions with and without 1000 mM NaCl, Anton Par MCR-302 rotational rheometer with concentric cylindrical geometries was used. Measurements were done at a shear rate range of 0.01 – 1.0 1/s with a parallel plate (25 mm diameter) geometry of the rheometer. Also, the apparent shear viscosity of all cellulose suspensions with 0.5 wt% concentration was performed by the DV3TLVTJ0 Brookfield rheometer. The shear rate was 50 1/s and the measuring time was 3 min with 6 measurements with a 30 seconds interval.

2.3. Emulsion Preparation and Stability Evaluation

2.3.1. Emulsion preparation

10 ml of cellulose suspension and dodecane with 2 mg Oil Blue dye were added to a 20 ml vial to prepare a 1:1 volume ratio emulsion. For CFs four different concentrations of 0.05, 0.1, 0.25 and 0.5 wt% were used. To compare the different celluloses, emulsions with 0.25 wt% of CNCs, CNFs, TEMPO-CNFs and CFs were prepared. The concentration here refers to the cellulose content in the emulsion phase. Therefore, the cellulose content in the used aqueous suspension is twice. To investigate the effect of salt and pH, modification of the salt concentration and pH were done on the aqueous phase before emulsification. Emulsification was performed using ultrasonication (Qsonica Q700) for about 1 minute at 100% amplitude to reach input energy of 3800 J. All the prepared emulsions were stored at ambient temperature for 14 days for stability analysis.

2.3.2. Visual assessment

The stability of the formulated emulsions in terms of dewatering/phase separation was evaluated by visual inspection of the stored emulsions. The inspection was performed after 1 day and 2, 3, 7 and 14 days after preparation of the emulsions. The serum and emulsion layer heights were recorded at these time intervals and the dewatering index was calculated based on the following formula:

$$DW = \frac{H_s}{H_a} \times 100 \quad (1)$$

Where H_s is the serum layer height separated from the emulsions phase at the bottom of the vials and H_a is the initial height of the aqueous phase in the vial.

2.3.3. Optical microscopy

To record the images of the oil droplets in the emulsions, a Zeiss Axio Vert.A1 optical microscope was used. A drop from each emulsion was deposited on a glass slide. Then a cover glass was laid on the top of the sample to avoid air bubbles and placed on the microscope. The obtained images were analyzed in Image J software to evaluate the droplets size distribution. The Sauter mean diameter ($D_{3,2}$)(Sauter 1926) of the droplets was obtained by evaluating at least 200 droplets. Sauter mean diameter ($D_{3,2}$) reflects the mean diameter of the droplets by taking into account the volume to surface area ratio and is calculated by the following equation:

$$D_{3,2} = \frac{\sum n_i d_i^3}{\sum n_i d_i^2} \quad (2)$$

Where d_i is the diameter of a droplet and n_i stands for the number of droplets.

To obtain the width of the droplets size distribution, the span (dispersion index) was calculated through the following formula (Mcclements 2007):

$$Span = \frac{d_{90} - d_{10}}{d_{50}} \quad (3)$$

where d_{10}, d_{50} and d_{90} are the droplet diameters that are larger than 10%, 50% and 90% of the droplets, respectively.

2.3.4. Fluorescent microscopy

The fluorescence images of the emulsions were taken using an Olympus IX73 inverted fluorescence microscope. CFs were labelled through incubation with CBM2a-eGFP. For this purpose, CFs were washed with 50 mM sodium phosphate buffer, pH 7.4. The liquid was removed by centrifuge. Then CFs were incubated with 0.26 mg/mL CBM2a-eGFP in 50 mM sodium phosphate buffer, pH 7.4 with gentle shaking overnight at 4°C. Excessive protein was removed by centrifugation. Protein-bound CFs were rinsed with sodium phosphate buffer, then resuspended in the same buffer for future application.

3. Results and Discussion

3.1. Characterization of different cellulose samples

To compare the different nanocellulose materials in terms of their surface charge and size, zeta potential and dynamic light scattering measurements were performed at neutral pH (Table 1). As

Table 1. Zeta potential and average apparent hydrodynamic diameter of the different celluloses

Cellulose	pH	Zeta potential (mV)	Average apparent hydrodynamic diameter (nm)
CNC	6.95	−30.42 ± 1.31	136.7 ± 30.3
CNF	6.8	−8.98 ± 3.39	2385 ± 411.5
TEMPO-CNF	6.93	−21.91 ± 2.16	220.3 ± 15.3
CF	6.97	−12.22 ± 0.65	3704 ± 324.1

186 expected, cellulose nanocrystal (CNC) showed a high negative surface charge (–30 mV) due to the
187 existence of sulfate groups resulting from their synthesis route which includes a sulfuric acid
188 hydrolysis step. Among the different nanocelluloses, cellulose nanofibrils (CNFs) and cellulose
189 filaments (CFs) have a low surface charge with a zeta potential of about –10 mV which is three
190 times lower than the CNCs. This is likely due to the mechanical refining methods used for their
191 preparation, which does not introduce extra acid groups on the fiber surface. The TEMPO oxidation
192 process in which the primary hydroxyl groups modified to anionic carboxylic groups results in
193 cellulose nanofibrils (TEMPO-CNFs) with a medium amount of negatively charged surface (–18
194 mV) among others. Aside from surface charges, the size of nanocelluloses is related to their
195 synthesis route, where CFs show the highest average apparent hydrodynamic diameter, followed
196 by CNF, TEMPO-CNFs and CNC. SEM image of the CFs (Figure S1) displays that CFs contain
197 both long and fine nano/microfibrillar materials demonstrating that why CFs average apparent
198 hydrodynamic diameter is larger than other types of nanocelluloses.

199 ## 3.2. Characterization of CF-Stabilized Emulsions

200 ### 3.2.1. Visual inspection

201 Visual inspections were carried out to evaluate the stability of the prepared emulsions by observing
202 their ability to resist physical changes over time. The photographs of the formulated emulsions at
203 various CFs concentrations immediately after preparation, 1 day after preparation and 14 days after
204 preparation are shown in Figure 1a – d. As seen from Figures 1a and 1b, the oil in water emulsions
205 prepared at 0.05 wt% and 0.1 wt% showed phase separation and creaming immediately after their
206 preparation. However, emulsions with CFs concentration of 0.25 wt% and 0.5 wt% exhibited a
207 delayed phase separation with a delay time of 1 day (Figures 1c and 1d). The emulsion volume
208 increased with the concentration of CF and at 0.5 wt% of CFs, there is almost complete

209 emulsification. Increasing CF concentrations allowed for increased droplet stabilization by
210 providing more interfaces that fill larger volumes. Additionally, higher CF concentration increases
211 viscosity, preventing mobilization of the continuous phase between the oil droplets, resulting in a
212 more stable emulsion. In Figures 1a and 1b, the cloudy serum layer at the bottom of the vials at CF
213 concentrations of 0.05 wt% and 0.1 wt% indicates that the CFs desorbed from the oil and water
214 interface and gathered in the serum layer. This is attributed to the high mobility of continuous phase
215 and coalescence of oil droplets resulting in detachment of the CFs from the interface. At CFs
216 concentrations of 0.25 wt% and 0.5 wt%, clear water is observed in the serum layer. This indicates
217 that all the particles are retained in the emulsion phase, either absorbed at the oil and water interface

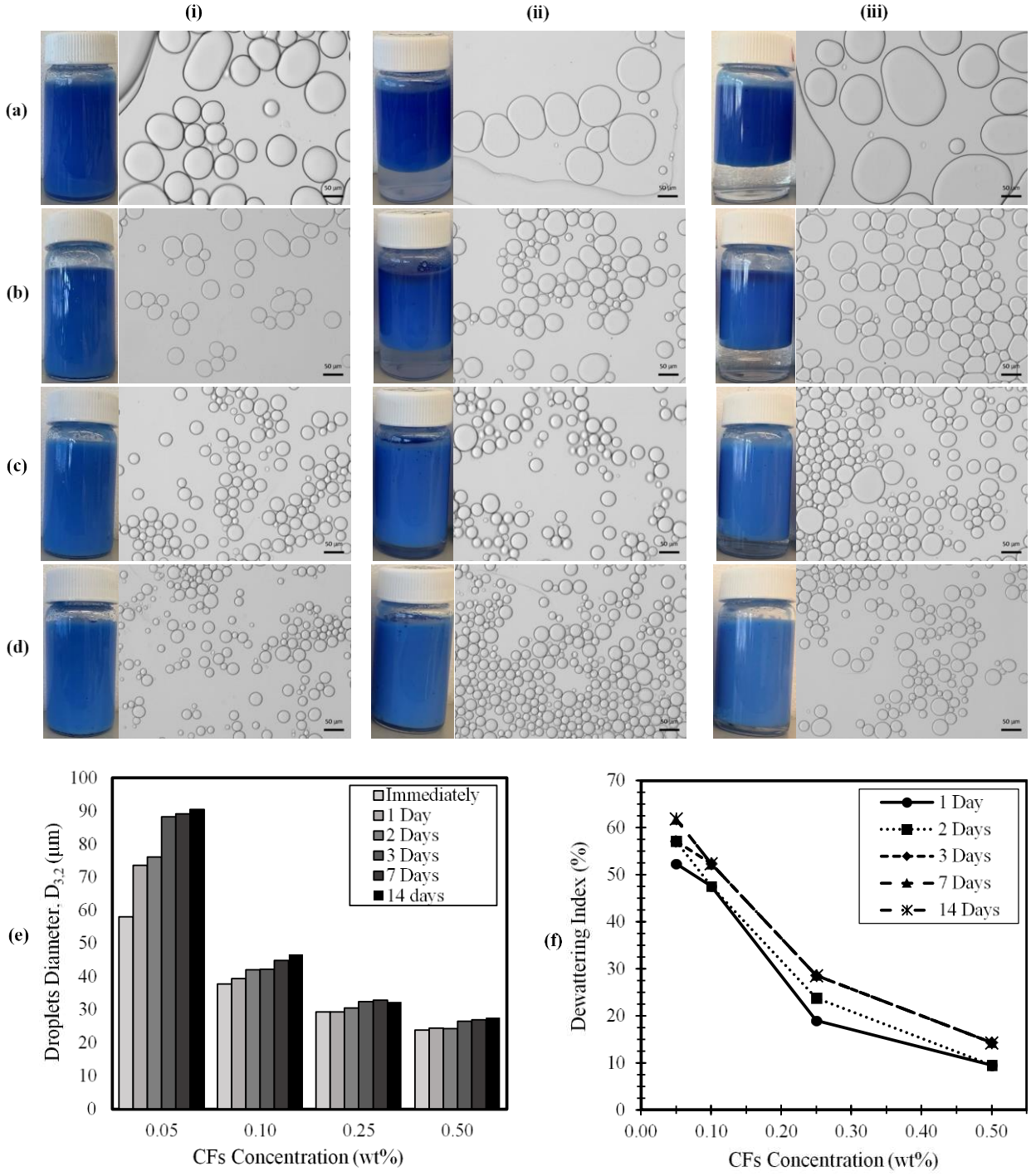

Figure 1. Photographs and optical microscope images at different CFs concentration and emulsion storage times (a) 0.05 wt% CFs, (b) 0.1 wt% CFs, (c) 0.25 wt% CFs, (d) 0.5 wt% CFs (i) immediately after preparation (ii) after 1 day of preparation and (iii) after 14 days of preparation; (e) average diameter of the droplets; (f) dewatering index of the emulsions

218 or retained in the continuous phase because of the low mobility of this phase and lack of droplet

coalescence. In general, photographs in Figures 1a – d show that CFs can stabilize oil in water emulsions with a concentration as low as 0.05 wt%, while the volume and stability of emulsion enhance with increasing concentration.

3.2.2. Droplets size distribution

The stability of the emulsions was evaluated by analyzing oil droplet morphology and the average diameter of droplets. In addition to the photographs of emulsions, the micrographs obtained by optical microscopy are also shown (Figures 1a – d). It appears that increasing the CF concentration from 0.05 wt% to 0.5 wt% leads to a clear reduction in droplet diameter. At very low concentrations of CF, there is obvious evidence of flocculation and coalescence. The degree of flocculation reduces as CFs concentration is increased to 0.1 wt% and 0.25 wt%. At CFs concentration of 0.5 wt% where the most stable emulsion is obtained, there is not much difference in the micrographs over time, indicating that at this concentration the emulsion is stable against flocculation and coalescence. In general, emulsions with smaller droplets demonstrate higher stability since it takes a longer time for the droplets to coalesce (Pal 1996). Quantitative analysis was performed by calculating the average diameter of the droplets ($d_{3,2}$) in Figure 1e. The average diameter of the droplets significantly increased over time at CFs concentration of 0.05 wt%, from a value of about 58 µm for fresh emulsions to 91 µm for emulsions stored for 14 days. At this concentration, the amount of CFs is too low to stabilize small droplets, resulting in a tendency to coalesce, reducing the total interface area of the system. By doubling the CFs concentration, the average diameter of the droplets became stable at a value of about 47 µm which is about half of the average diameter of the droplets at 0.05 wt% CFs. By increasing the CF concentration both the average diameter of the droplets and the percent of change in its value with the storage period reduce. For the emulsions with 0.5 wt% CF, there is only a negligible increase in the average diameter of droplets after 14

days, demonstrating good stability of the emulsions. The size distribution of the droplets for all the emulsions are provided in Figures S2 – S5. Additionally, the span of the emulsions reduced from a value of 2.2 at 0.05 wt% CFs to a value of 0.73 at 0.5 wt% CFs, indicating very wide droplets size distribution at low concentration as a result of significant coalescence. Increased CFs concentration led to a decrease in droplet size distribution range. Span index calculations are summarized in Table S1.

3.2.3. Dewatering Index

The stability of the emulsions was further evaluated by analyzing the dewatering index. The calculated dewatering index based on visual inspection (Figure 1f) shows that the phase separation of the water phase from the emulsion starts shortly after the generation of the emulsions. Most of the dewatering happened within a day after emulsion preparation, independent of the amount of CFs introduced. After one day, the dewatering index slightly increased, reaching a constant value after three days for all emulsions. The most stable emulsion is the emulsion with 0.5 wt% of CFs which is stabilized at a dewatering index of 14%. In the case of emulsions with 0.05 and 0.1 wt% CFs, more than 50% of the water in the emulsion dewatered after 14 days which can be attributed to two effects: (i) larger droplet size and (ii) lower continuous phase viscosity.

3.3. Fluorescent Microscopy

To better understand the mechanism of CFs stabilizing oil-water emulsion, fluorescent protein labelled carbohydrate-binding module (CBM) was employed to visualize the location of CFs under the fluorescent microscope. CBMs are the special structural protein modules of carbohydrate-active enzymes, which play the role of binding the enzymes to their targeted polysaccharides in nature. The high binding specificity and the relatively simple operation endow CBMs with excellent potential to probe the carbohydrate polymers in a complex system. We and others have

265 developed various engineered CBM linked with different fluorescent proteins/probes to assess the
266 location and/or surface morphology of various cellulosic fibers in recent years (Gourlay et al. 2015;
267 Hébert-Ouellet et al. 2017; Long et al. 2019).

268 In this study, the specific cellulose-binding carbohydrate-binding module (CBM2a) linked with
269 enhanced Green fluorescent protein (CBM2a-eGFP) was used to track the location of CFs within

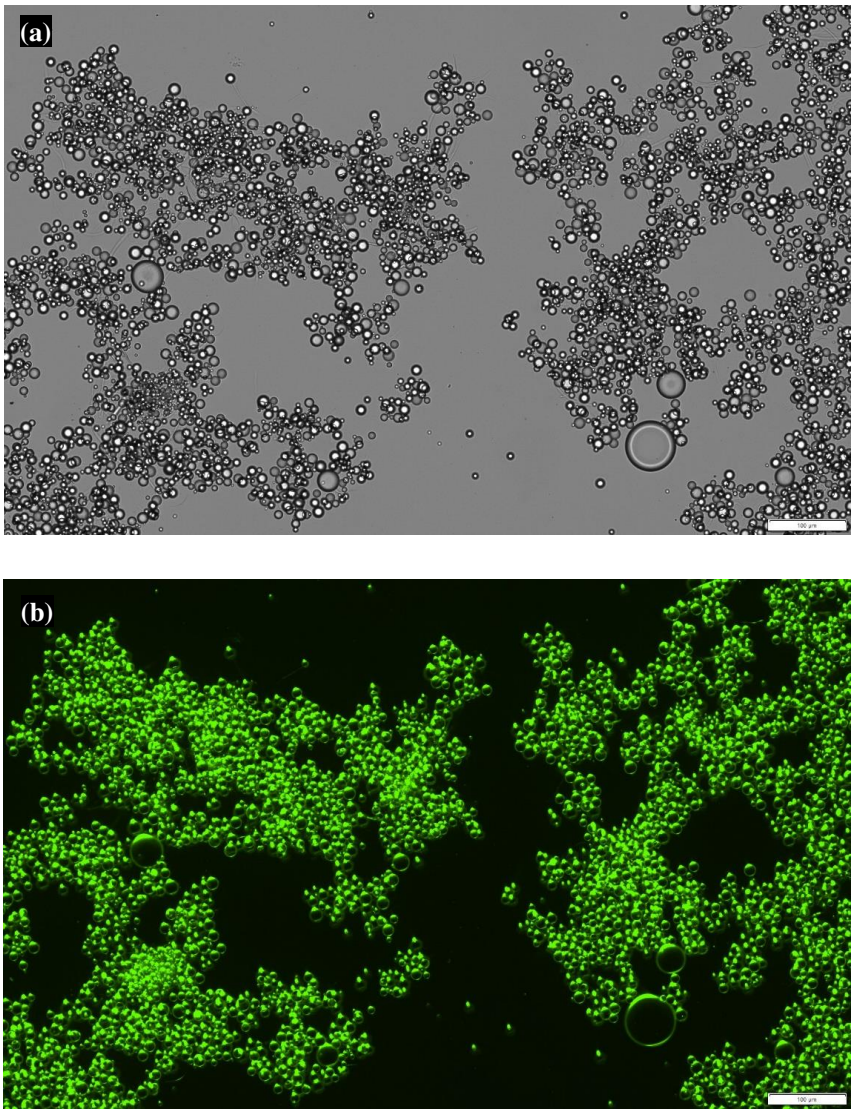

Figure 2. Fluorescent microscope images of the emulsion prepared with 0.5wt% CFs, (a) bright-field (b): fluorescent light (scale bar is 100 µm), note CFs are found entirely at droplet surfaces.

the emulsion. Figure 2 displays the fluorescent microscope images of the stabilized emulsions with 0.5 wt% CFs labelled by CBM2a-eGFP under bright field and fluorescent light. The fluorescent light images in Figure 2b (corresponding to the bright field image in Figure 2a) displays the adsorption of the CFs at the oil and water interface. The bright fluorescent light can be observed around the oil droplets while the inside of the droplets is dark. Also, no fluorescent reflection was observed in the continuous phase. This observation indicates the mechanism of stabilizing emulsions by CFs. CFs are mainly located at the oil and water interface demonstrating their adsorption at the oil droplet surfaces, leading to particle-stabilized Pickering emulsions.

3.4. Effect of Ionic Strength

It has been demonstrated that changing the ionic strength can greatly affect the stability of Pickering emulsions. In this study, the effect of the addition of simple electrolyte, NaCl on the CFs suspension zeta potential (Figure 3a), on the 0.5 wt% CF-stabilized emulsion stability (in terms of the average diameter of droplets and dewatering index (Figure 3b and 3c)), and on the viscosity of CFs suspensions (Figure 3d) are investigated, respectively. Figure 3a displays that the zeta potential of CFs suspension is reduced from a value of −18 mV to a value of about −6 mV in the presence of 60 mM NaCl, which is due to the electric double layer formed by the addition of Na^+ cation counter ions. The Na^+ counter ions adsorb to the CF particles' surface shielding their surface charge and causing a reduction in the electrostatic repulsion, therefore reducing the zeta potential value. The electrostatic screening happens in the presence of Na^+ counter ions and the Debye-Huckel screening strength expands by increasing Na^+ counter ions concentration hence Debye length decreases.(Prathapan et al. 2016)

Unlike Zeta potential, the addition of NaCl (100 mM) initially increases the average diameter of oil droplets and then decreases the droplet size as salt concentration is increased to 500

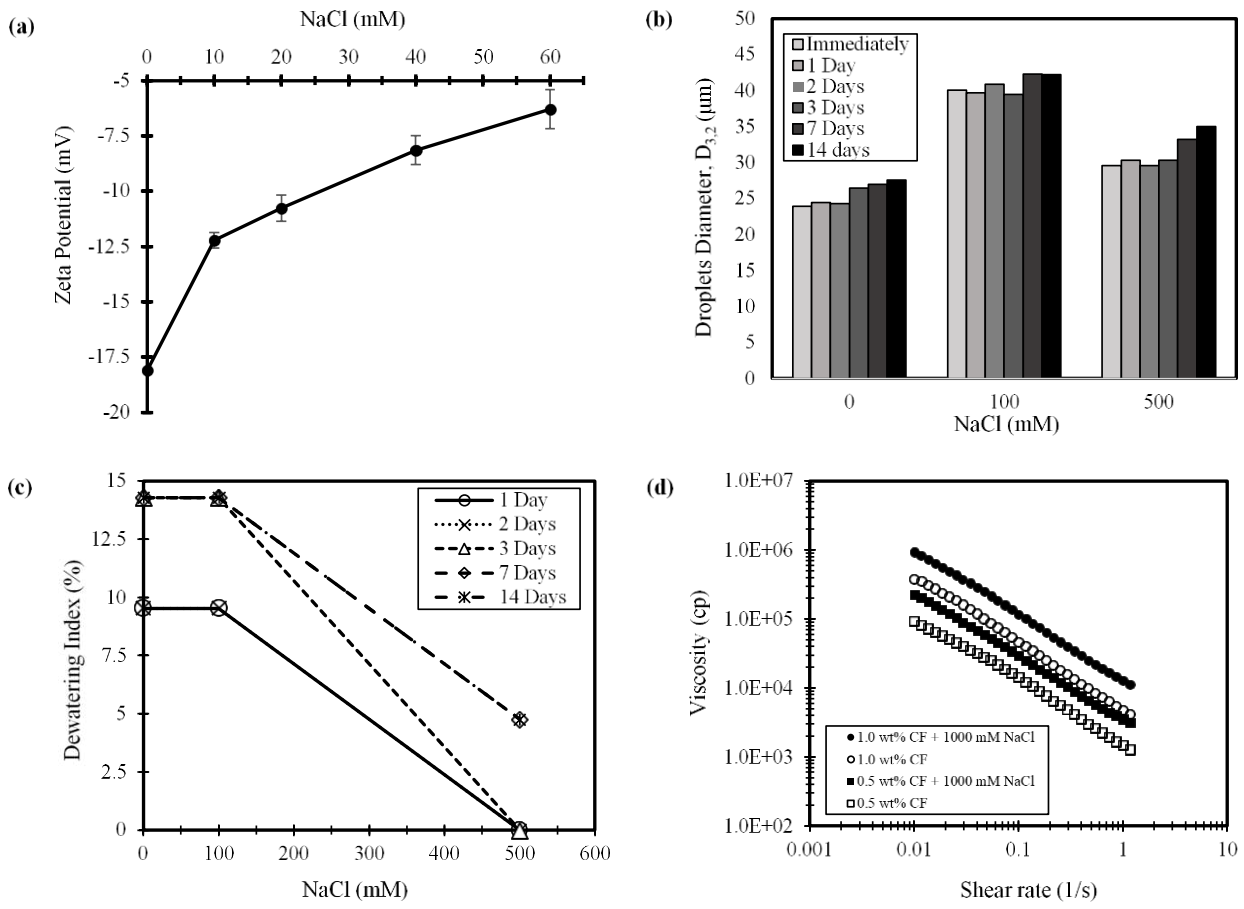

Figure 3. Effect of salt (a) on the zeta potential of CFs suspension at pH of 7 (b) on the average diameter of the droplets ($D_{3,2}$) of the stabilized O/W emulsions with CF concentration of 0.5 wt%, (c) on the average dewatering index of the stabilized O/W emulsions with CF concentration of 0.5 wt%, (d) on the viscosity of CFs suspensions

mM. (Figure 3b). The increasing droplet diameter in the presence of 100 mM NaCl could be attributed to the reduction in the electrostatic repulsion between the droplets allowing flocculation to take place, as evidenced by reducing Zeta Potential in Figure 3a. The reduction of the droplet diameter by the addition of more NaCl to the system (500 mM NaCl) appears to be related to the enhanced viscosity at this salt concentration. This will be discussed in more detail later (Figure 3d). Although the droplet size increased (Figure 3b), the dewatering index remains constant after the

addition of 100 mM NaCl to the system (Figure 3c). However, in the presence of 500 mM NaCl, the dewatering index slightly decreased which indicates better stability of the emulsion with high salt concentration. At both CF concentrations of 0.5 and 1.0 wt%, the addition of 1000 mM NaCl to the suspension (equivalent to the presence of 500 mM NaCl in the emulsion) increases the viscosity of suspensions by a factor of two (Figure 3d). It seems that the enhanced viscosity of the continuous phase in the presence of high salt concentration helps the stability of emulsions by immobilizing the droplets and preventing them from flocculation. In general, from Figure 3, it can be seen that the presence of salts does not significantly affect the stability of CF stabilized oil in water emulsions, and these emulsions are stable over a wide range of ionic strengths.

3.5. Effect of pH

To further investigate the effect of pH variation on CF stabilized oil in water emulsions, the zeta potential of CFs suspension, the average diameter of droplets and the dewatering index of the emulsions are next assessed at different pH (Figure 4). By reducing the pH from 10 to about 1.88, the zeta potential of the CFs suspension is reduced from a value of −15.5 mV to a value of near zero (Figure 4a). This is likely because of the protonation of the negative surfaces (carboxyl and hydroxyl groups) by the addition of acid to the systems, which reduces the total surface charge density of the CFs. Figure 4b and 4c show the effect of pH on the stability of the emulsion at 0.25 wt% and 0.5 wt% CFs concentration. The average diameter of the oil droplets slightly reduced as pH was increased, as the surface charge protonation at low pH reduces the repulsion between the droplets which causes more droplets interactions and results in the increased diameter. However, the formulated emulsions are fairly independent of the pH as the dewatering index remained almost constant at all pH values. This indicates that changing the pH did not trigger phase separation and further demonstrates the strong adsorption of CF particles to the oil and water interface.

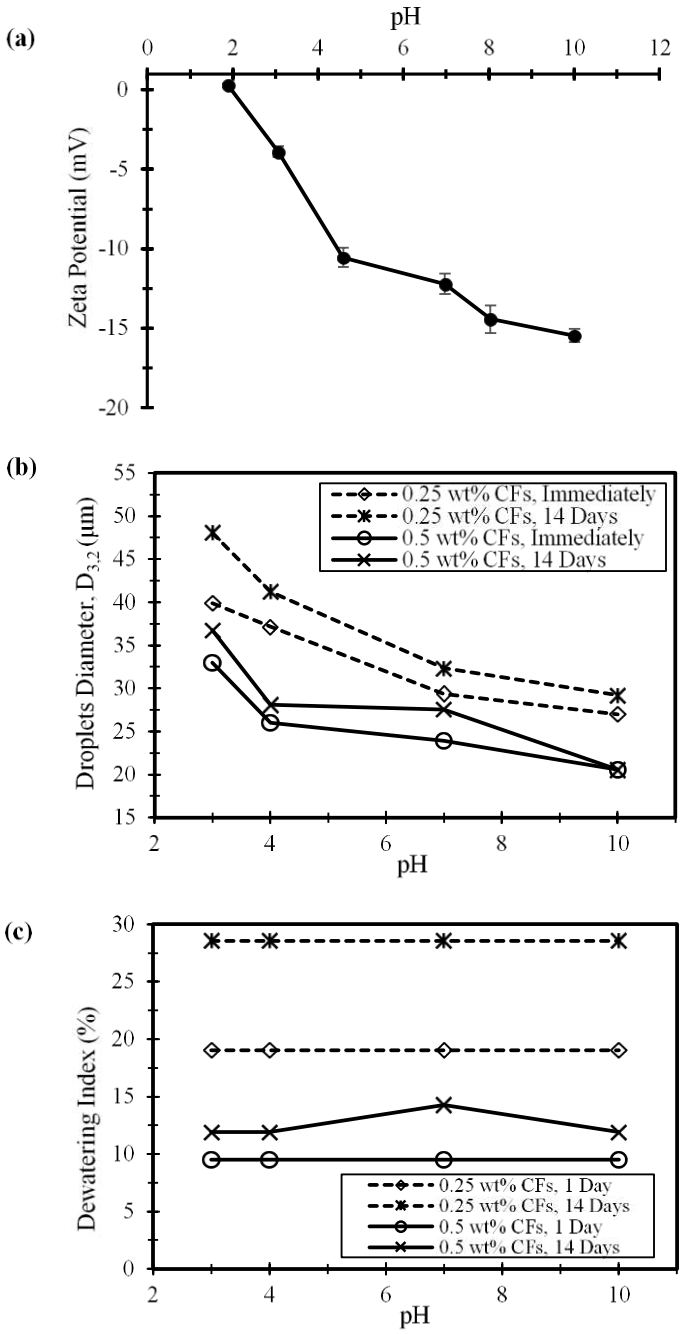

Figure 4. Effect of pH (a) on the zeta potential of CFs suspension with 10mM NaCl, (b) on the average diameter of the droplets ($D_{3,2}$) of the stabilized O/W emulsions with CF stabilized O/W emulsions with CFs concentrations of 0.25 wt% and 0.5 wt%, (c) and on the dewatering index of the stabilized O/W emulsions with CFs concentrations of 0.25 wt% and 0.5 wt%

322

3.6. Comparison of the different types of celluloses

To compare the ability of different types of celluloses in stabilizing oil in water emulsions, four emulsions with 0.25 wt% concentration of CNCs, CNFs, TMPO-CNFs and CFs are formulated. All the investigated different cellulose particles can provide stable emulsions. However, as can be seen from Figure 5a and 5b, the emulsion stabilized by TEMPO-CNFs has the smallest droplet size, while the CFs stabilized emulsions have the largest droplets. Dewatering index results (Figure 5c) show that the CNFs can provide the highest emulsion volume (lowest dewatering index) followed by CFs, TEMPO-CNFs and CNCs. This may be attributed to the adsorption energy of the

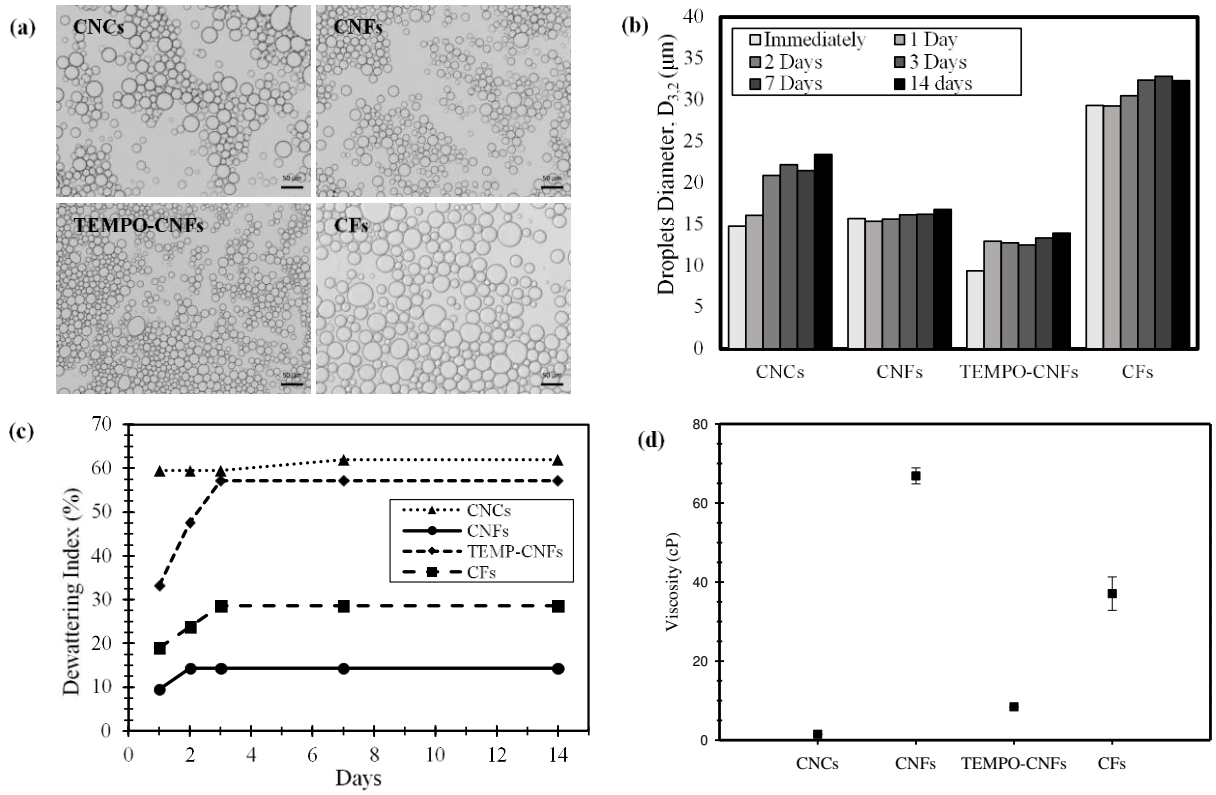

Figure 5. Comparison of the capability of different celluloses on stabilizing O/W emulsions at particle concentration of 0.25 wt% (a) microscope images of the stabilized emulsions, (b) average diameter of the droplets ($D_{3,2}$), (c) dewatering index, (d) viscosity of suspensions with 0.5 wt% concentration at a shear rate of 50 1/s.

particles. Adsorption of CFs and CNFs to the interface appears to be stronger and irreversible, while adsorption of CNCs and TEMPO-CNFs is reversible. These celluloses desorbed from the interface leading most of the emulsion phase to become unstable shortly after preparation. Another explanation for the higher stability of emulsions stabilized by CFs and CNFs in comparison to CNCs and TEMPO-CNFs is that CFs and CNFs suspensions have higher viscosity (Figure 5d).

Overall, considering the much cheaper production cost of CFs and the stable Pickering emulsion it forms at varying salt concentrations and pH, CFs can be a better choice than other nanocellulose materials for stabilizing emulsions for a wide range of applications.

4. Conclusions

In this study, the potential application of a novel and green material, cellulose filaments (CFs) in stabilizing oil in water Pickering emulsions is investigated. Because of the strong adsorption of the CFs to the oil and water interface and formation of a highly viscous aqueous phase, CFs successfully stabilized oil in water emulsions. In contrast to CFs, emulsions stabilized by CNCs and TEMPO-CNFs showed significant coalescence and creaming even though they have smaller average droplets diameter. Results showed that the better performance of the CFs was likely due to the high viscosity of the aqueous phase in the presence of CFs compared to CNCs and TEMPO-CNFs. The analysis of the effects of pH and salt concentration showed that the CFs-stabilized emulsion was not significantly affected by a change in the pH (2 – 10) and salt concentrations (0 – 500 mM). From the results presented here, it can be concluded that the CFs are a promising new nanocellulose for the sustainable and cost-efficient formulation of stable Pickering emulsions without using any additives or surfactants and with potential applications in a wide range of markets.

Acknowledgements

This work is financially supported by the Canada First Research Excellence Fund (CFREF).

Declarations:

Compliance with ethical standards

Conflict of interest The authors declare that they have no conflict of interest.

References

Aaen R, Brodin FW, Simon S, et al (2019) Oil-in-Water Emulsions Stabilized by Cellulose Nanofibrils-The Effects of Ionic Strength and pH. Nanomater (Basel, Switzerland) 9:259. https://doi.org/10.3390/nano9020259

Ahmad AL, Zaulkiflee ND, Kusumastuti A, Buddin MMHS (2019) Removal of Acetaminophen from Aqueous Solution by Emulsion Liquid Membrane: Emulsion Stability Study. Ind Eng Chem Res 58:713–719. https://doi.org/10.1021/acs.iecr.8b03562

Bai L, Lv S, Xiang W, et al (2019) Oil-in-water Pickering emulsions via microfluidization with cellulose nanocrystals: 1. Formation and stability. Food Hydrocoll 96:699–708. https://doi.org/https://doi.org/10.1016/j.foodhyd.2019.04.038

Björkegren S, Freixiela Dias MCA, Lundahl K, et al (2020) Phase Inversions Observed in Thermoresponsive Pickering Emulsions Stabilized by Surface Functionalized Colloidal Silica. Langmuir 36:2357–2367. https://doi.org/10.1021/acs.langmuir.9b03648

D'Acierno F, Hamad WY, Michal CA, MacLachlan MJ (2020) Thermal Degradation of Cellulose Filaments and Nanocrystals. Biomacromolecules 21:3374–3386. https://doi.org/10.1021/acs.biomac.0c00805

Fessi N, Nsib MF, Chevalier Y, et al (2019) Photocatalytic Degradation Enhancement in Pickering Emulsions Stabilized by Solid Particles of Bare TiO2. Langmuir 35:2129–2136. https://doi.org/10.1021/acs.langmuir.8b03806

Ghosh P (2009) Colloid and interface science. PHI Learning Pvt. Ltd.

Gonzalez Ortiz D, Pochat-Bohatier C, Cambedouzou J, et al (2020) Current Trends in Pickering Emulsions: Particle Morphology and Applications. Engineering 6:468–482. https://doi.org/https://doi.org/10.1016/j.eng.2019.08.017

Gourlay K, Hu J, Arantes V, et al (2015) The use of carbohydrate binding modules (CBMs) to monitor changes in fragmentation and cellulose fiber surface morphology during cellulase-and swollenin-induced deconstruction of lignocellulosic substrates. J Biol Chem 290:2938–2945

Hamad WY, Miao C, Beck S (2019) Growing the Bioeconomy: Advances in the Development of Applications for Cellulose Filaments and Nanocrystals. Ind Biotechnol 15:133–137

He Y, Wu F, Sun X, et al (2013) Factors that Affect Pickering Emulsions Stabilized by Graphene Oxide. ACS Appl Mater Interfaces 5:4843–4855. https://doi.org/10.1021/am400582n

Hébert-Ouellet Y, Meddeb-Mouelhi F, Khatri V, et al (2017) Tracking and predicting wood fibers processing with fluorescent carbohydrate binding modules. Green Chem 19:2603–2611

Hu J, Arantes V, Pribowo A, et al (2014) Substrate factors that influence the synergistic interaction of AA9 and cellulases during the enzymatic hydrolysis of biomass. Energy Environ Sci 7:2308–2315

Jiang H, Sheng Y, Ngai T (2020) Pickering emulsions: Versatility of colloidal particles and recent applications. Curr Opin Colloid Interface Sci 49:1–15. https://doi.org/https://doi.org/10.1016/j.cocis.2020.04.010

Jiang Y, Zhang Y, Ding L, et al (2019) Regenerated cellulose-dispersed polystyrene composites enabled via Pickering emulsion polymerization. Carbohydr Polym 223:115079. https://doi.org/https://doi.org/10.1016/j.carbpol.2019.115079

Jiménez-Saelices C, Trongsatitkul T, Lourdin D, Capron I (2020) Chitin Pickering Emulsion for Oil Inclusion in Composite Films. Carbohydr Polym 242:116366. https://doi.org/https://doi.org/10.1016/j.carbpol.2020.116366

Khan A, Wen Y, Huq T, Ni Y (2018) Cellulosic Nanomaterials in Food and Nutraceutical Applications: A Review. J Agric Food Chem 66:8–19. https://doi.org/10.1021/acs.jafc.7b04204

Kiss N, Brenn G, Pucher H, et al (2011) Formation of O/W emulsions by static mixers for pharmaceutical applications. Chem Eng Sci 66:5084–5094. https://doi.org/https://doi.org/10.1016/j.ces.2011.06.065

Lee MC, Dadmohammadi Y, Tan C, Abbaspourrad A (2020) Mitigating the Astringency of Acidified Whey Protein in Proteinaceous High Internal Phase Emulsions. ACS Appl Bio Mater 3:8438–8445. https://doi.org/10.1021/acsabm.0c00767

Li W, Suzuki T, Minami H (2019) The interface adsorption behavior in a Pickering emulsion stabilized by cylindrical polystyrene particles. J Colloid Interface Sci 552:230–235. https://doi.org/https://doi.org/10.1016/j.jcis.2019.05.058

Li Z, Wu H, Yang M, et al (2018) Stability mechanism of O/W Pickering emulsions stabilized with regenerated cellulose. Carbohydr Polym 181:224–233.

https://doi.org/https://doi.org/10.1016/j.carbpol.2017.10.080

Long L, Hu J, Li X, et al (2019) The Potential of Using Thermostable Xylan-Binding Domain as a Molecular Probe to Better Understand the Xylan Distribution of Cellulosic Fibers. ACS Sustain Chem Eng 7:12520–12526

Low LE, Siva SP, Ho YK, et al (2020) Recent advances of characterization techniques for the formation, physical properties and stability of Pickering emulsion. Adv Colloid Interface Sci 277:102117. https://doi.org/https://doi.org/10.1016/j.cis.2020.102117

Marto J, Pinto P, Fitas M, et al (2018) Safety assessment of starch-based personal care products: Nanocapsules and pickering emulsions. Toxicol Appl Pharmacol 342:14–21. https://doi.org/https://doi.org/10.1016/j.taap.2018.01.018

Mcclements DJ (2007) Critical Review of Techniques and Methodologies for Characterization of Emulsion Stability. Crit Rev Food Sci Nutr 47:611–649. https://doi.org/10.1080/10408390701289292

Mikulcová V, Bordes R, Minařík A, Kašpárková V (2018) Pickering oil-in-water emulsions stabilized by carboxylated cellulose nanocrystals – Effect of the pH. Food Hydrocoll 80:60–67. https://doi.org/https://doi.org/10.1016/j.foodhyd.2018.01.034

Pal R (1996) Effect of droplet size on the rheology of emulsions. AIChE J 42:3181–3190. https://doi.org/10.1002/aic.690421119

Pandey A, Derakhshandeh M, Kedzior SA, et al (2018a) Role of interparticle interactions on microstructural and rheological properties of cellulose nanocrystal stabilized emulsions. J Colloid Interface Sci 532:808–818. https://doi.org/https://doi.org/10.1016/j.jcis.2018.08.044

Pandey A, Telmadarreie A, Trifkovic M, Bryant S (2018b) Cellulose Nanocrystal Stabilized Emulsions for Conformance Control and Fluid Diversion in Porous Media. SPE Annu. Tech. Conf. Exhib. 18

Pickering SU (1907) Cxcvi.—emulsions. J Chem Soc Trans 91:2001–2021

Prathapan R, Thapa R, Garnier G, Tabor RF (2016) Modulating the zeta potential of cellulose nanocrystals using salts and surfactants. Colloids Surfaces A Physicochem Eng Asp 509:11–18. https://doi.org/https://doi.org/10.1016/j.colsurfa.2016.08.075

Ragesh P, Ganesh VA, Nair S V, Nair AS (2014) A review on 'self-cleaning and multifunctional materials.' J Mater Chem A 2:14773–14797

Ramsden W (1904) Separation of solids in the surface-layers of solutions and 'suspensions'(observations on surface-membranes, bubbles, emulsions, and mechanical coagulation).—Preliminary account. Proc R Soc London 72:156–164

Sauter J (1926) Die Grössenbestimmung der im Gemischnebel von Verbrennungskraftmaschinen vorhandenen Brennstoffteilchen:(Mitteilung aus d. Labor. f. techn. Physik d. Techn. Hochsch. München); mit 26 Abb. u. 8 Zahlentaf. VDI-Verlag

Schramm LL (2014) Emulsions, foams, suspensions, and aerosols: microscience and applications. John Wiley & Sons

Shao P, Feng J, Sun P, et al (2020) Recent advances in improving stability of food emulsion by plant polysaccharides. Food Res Int 137:109376. https://doi.org/https://doi.org/10.1016/j.foodres.2020.109376

Shi A, Feng X, Wang Q, Adhikari B (2020) Pickering and high internal phase Pickering emulsions stabilized by protein-based particles: A review of synthesis, application and prospective. Food Hydrocoll 109:106117. https://doi.org/https://doi.org/10.1016/j.foodhyd.2020.106117

Varanasi S, Henzel L, Mendoza L, et al (2018) Pickering Emulsions Electrostatically Stabilized by Cellulose Nanocrystals . Front. Chem. 6:409

Venkataramani D, Tsulaia A, Amin S (2020) Fundamentals and applications of particle stabilized emulsions in cosmetic formulations. Adv Colloid Interface Sci 283:102234. https://doi.org/https://doi.org/10.1016/j.cis.2020.102234

Wu F, Deng J, Hu L, et al (2020) Investigation of the stability in Pickering emulsions preparation with commercial cosmetic ingredients. Colloids Surfaces A Physicochem Eng Asp 602:125082. https://doi.org/https://doi.org/10.1016/j.colsurfa.2020.125082

Xie C-Y, Meng S-X, Xue L-H, et al (2017) Light and Magnetic Dual-Responsive Pickering Emulsion Micro-Reactors. Langmuir 33:14139–14148. https://doi.org/10.1021/acs.langmuir.7b03642

Xue F, Zhang Y, Zhang F, et al (2017) Tuning the Interfacial Activity of Mesoporous Silicas for Biphasic Interface Catalysis Reactions. ACS Appl Mater Interfaces 9:8403–8412. https://doi.org/10.1021/acsami.6b16605

Yan H, Chen X, Feng M, et al (2019) Entrapment of bacterial cellulose nanocrystals stabilized Pickering emulsions droplets in alginate beads for hydrophobic drug delivery. Colloids Surfaces B Biointerfaces 177:112–120. https://doi.org/https://doi.org/10.1016/j.colsurfb.2019.01.057

Yan X, Ma C, Cui F, et al (2020) Protein-stabilized Pickering emulsions: Formation, stability, properties, and applications in foods. Trends Food Sci Technol 103:293–303. https://doi.org/https://doi.org/10.1016/j.tifs.2020.07.005

Zhang R, Belwal T, Li L, et al (2020) Recent advances in polysaccharides stabilized emulsions for encapsulation and delivery of bioactive food ingredients: A review. Carbohydr Polym 242:116388. https://doi.org/https://doi.org/10.1016/j.carbpol.2020.116388

Zhang X, Wang Y, Luo X, et al (2019) O/W Pickering Emulsion Templated Organo-hydrogels with Enhanced Mechanical Strength and Energy Storage Capacity. ACS Appl Bio Mater 2:480–487. https://doi.org/10.1021/acsabm.8b00674

Zhao D, Yu D, Kim M, et al (2019) Effects of temperature, light, and pH on the stability of fucoxanthin in an oil-in-water emulsion. Food Chem 291:87–93. https://doi.org/https://doi.org/10.1016/j.foodchem.2019.04.002

Zhou Y, Yin D, Chen W, et al (2019) A comprehensive review of emulsion and its field application for enhanced oil recovery. Energy Sci Eng 7:1046–1058. https://doi.org/10.1002/ese3.354

Zhu F (2019) Starch based Pickering emulsions: Fabrication, properties, and applications. Trends Food Sci Technol 85:129–137. https://doi.org/https://doi.org/10.1016/j.tifs.2019.01.012

Zhu Y, Lu L-H, Gao J, et al (2013) Effect of trace impurities in triglyceride oils on phase inversion of Pickering emulsions stabilized by CaCO3 nanoparticles. Colloids Surfaces A Physicochem Eng Asp 417:126–132. https://doi.org/https://doi.org/10.1016/j.colsurfa.2012.10.043

Figures

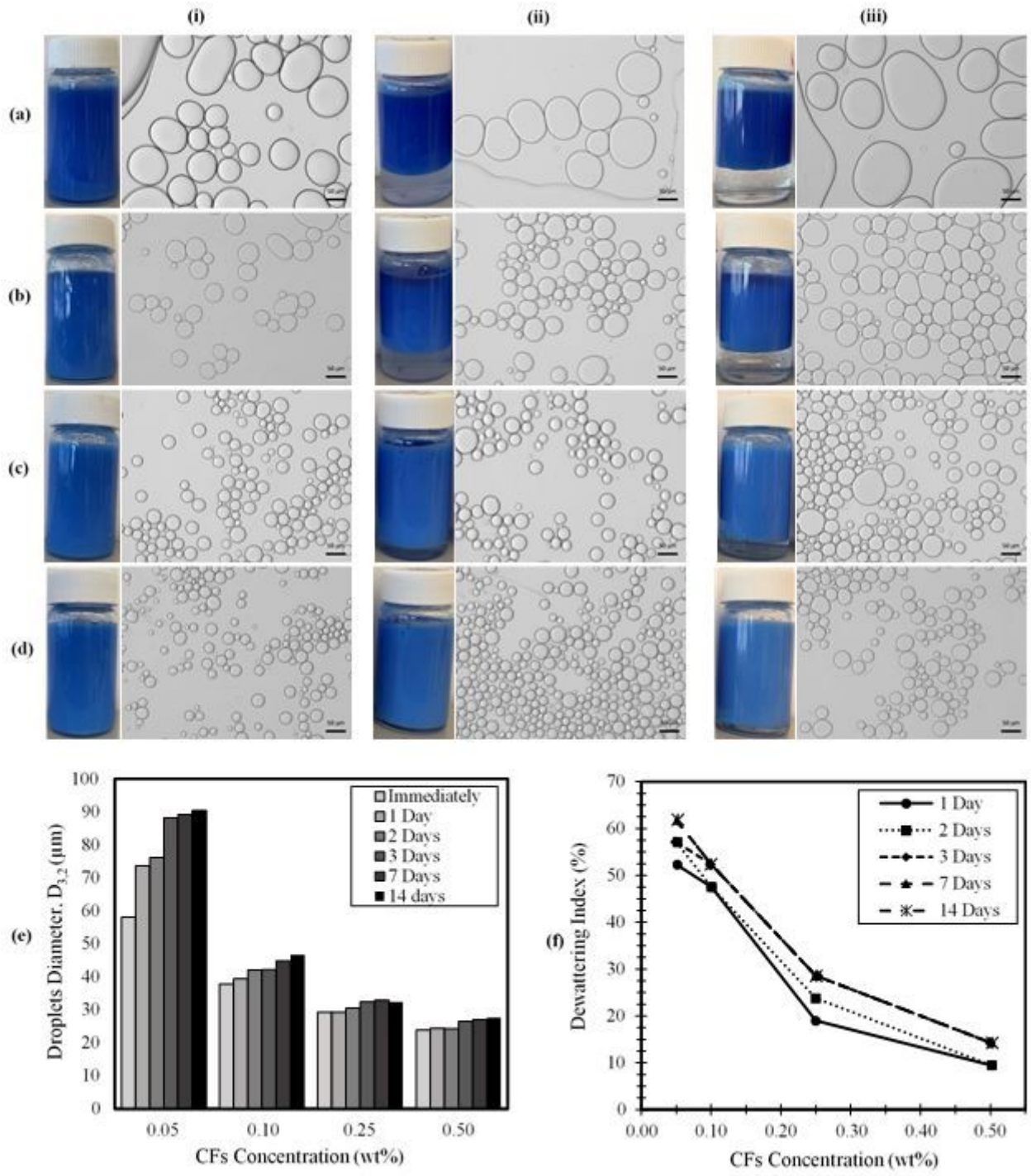

Figure 1

Photographs and optical microscope images at different CFs concentration and emulsion storage times (a) 0.05 wt% CFs, (b) 0.1 wt% CFs, (c) 0.25 wt% CFs, (d) 0.5 wt% CFs (i) immediately after preparation (ii) after 1 day of preparation and (iii) after 14 days of preparation; (e) average diameter of the droplets; (f) dewatering index of the emulsions

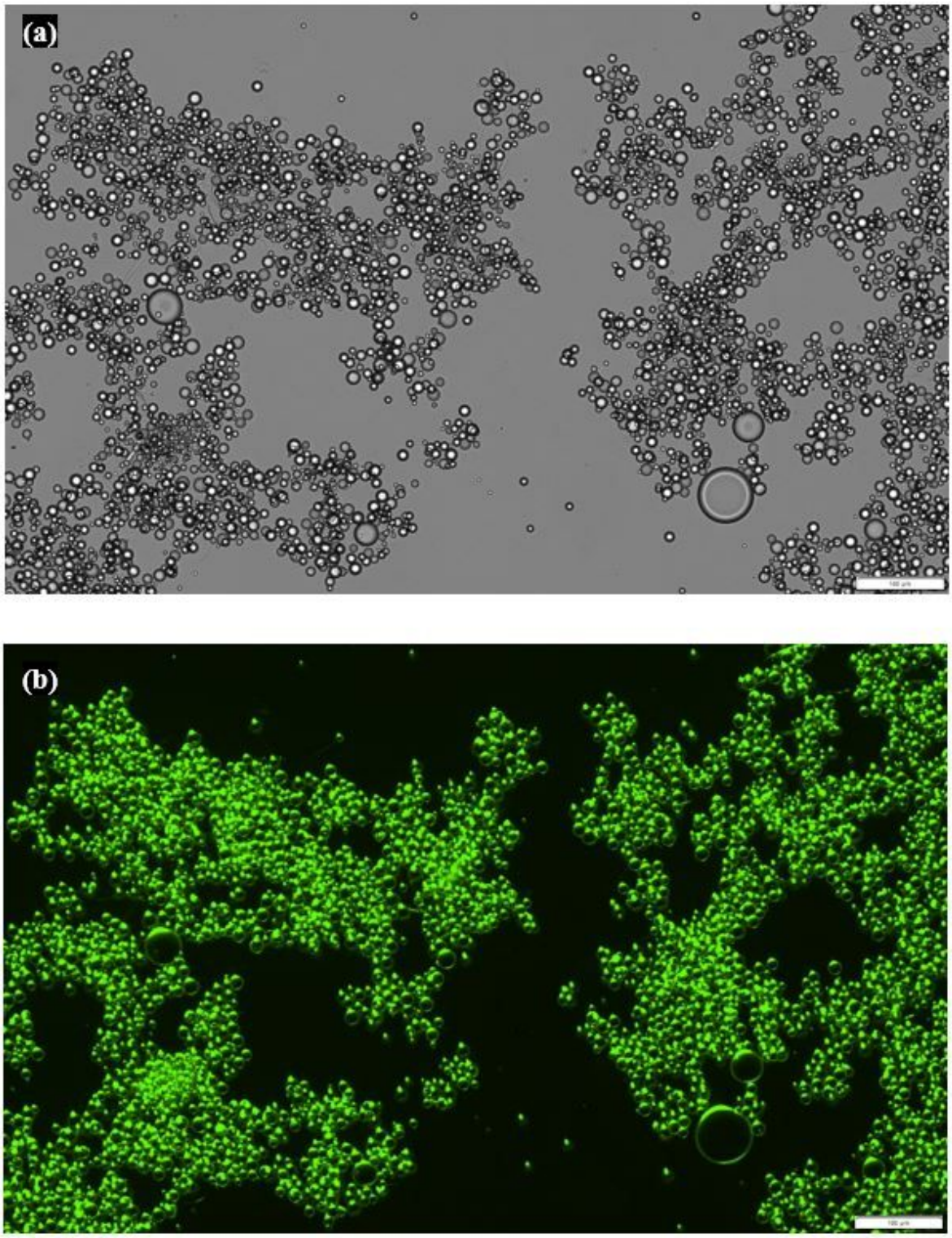

Figure 2

Fluorescent microscope images of the emulsion prepared with 0.5wt% CFs, (a) bright-field (b): fluorescent light (scale bar is 100 μm), note CFs are found entirely at droplet surfaces.

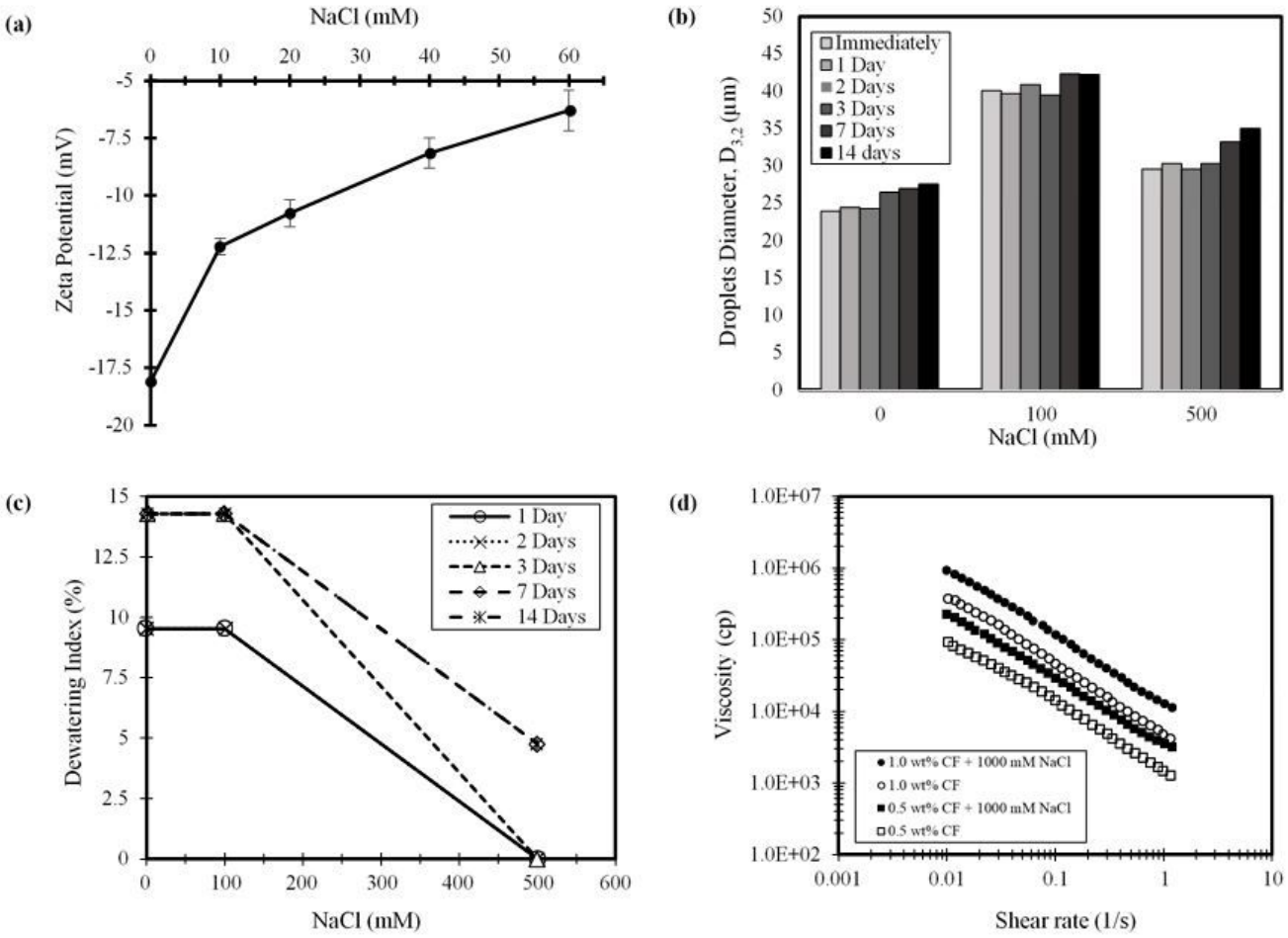

Figure 3

Effect of salt (a) on the zeta potential of CFs suspension at pH of 7 (b) on the average diameter of the droplets (D3, 2) of the stabilized O/W emulsions with CF concentration of 0.5 wt%, (c) on the average dewatering index of the stabilized O/W emulsions with CF concentration of 0.5 wt%, (d) on the viscosity of CFs suspensions

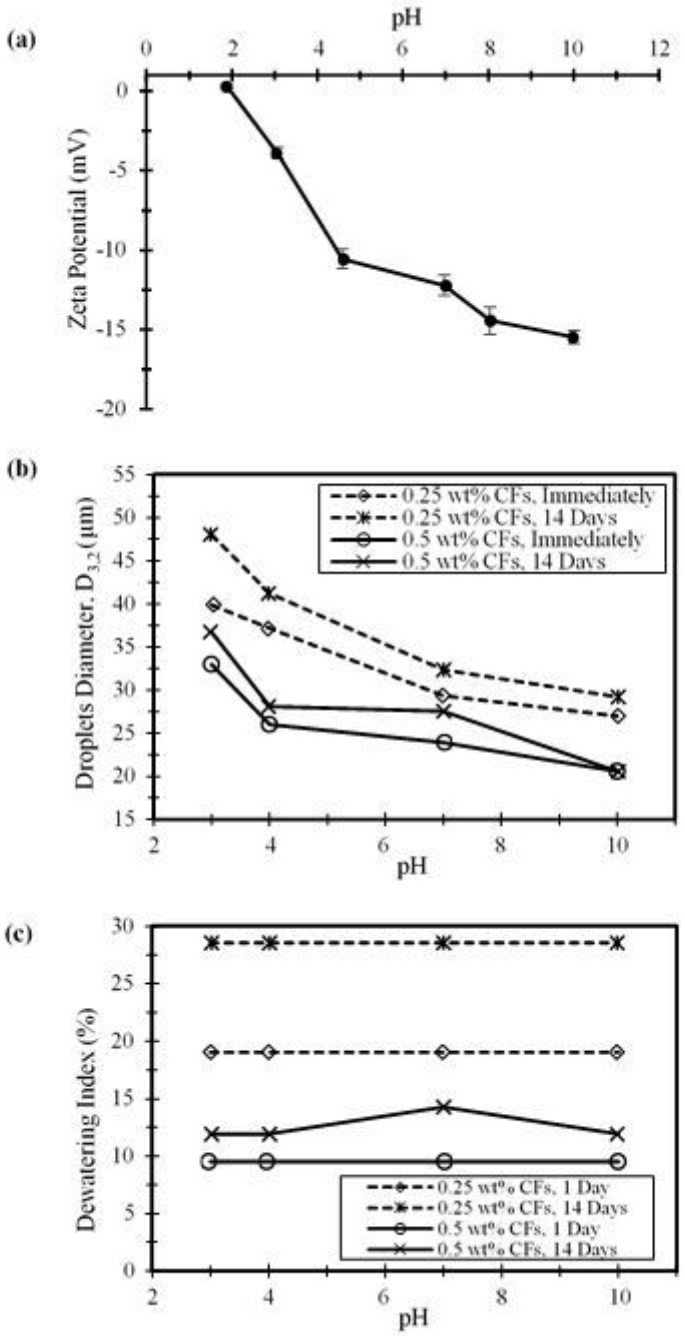

Figure 4

Effect of pH (a) on the zeta potential of CFs suspension with 10mM NaCl, (b) on the average diameter of the droplets (D3, 2) of the stabilized O/W emulsions with CF stabilized O/W emulsions with CFs concentrations of 0.25 wt% and 0.5 wt%, (c) and on the dewatering index of the stabilized O/W emulsions with CFs concentrations of 0.25 wt% and 0.5 wt%

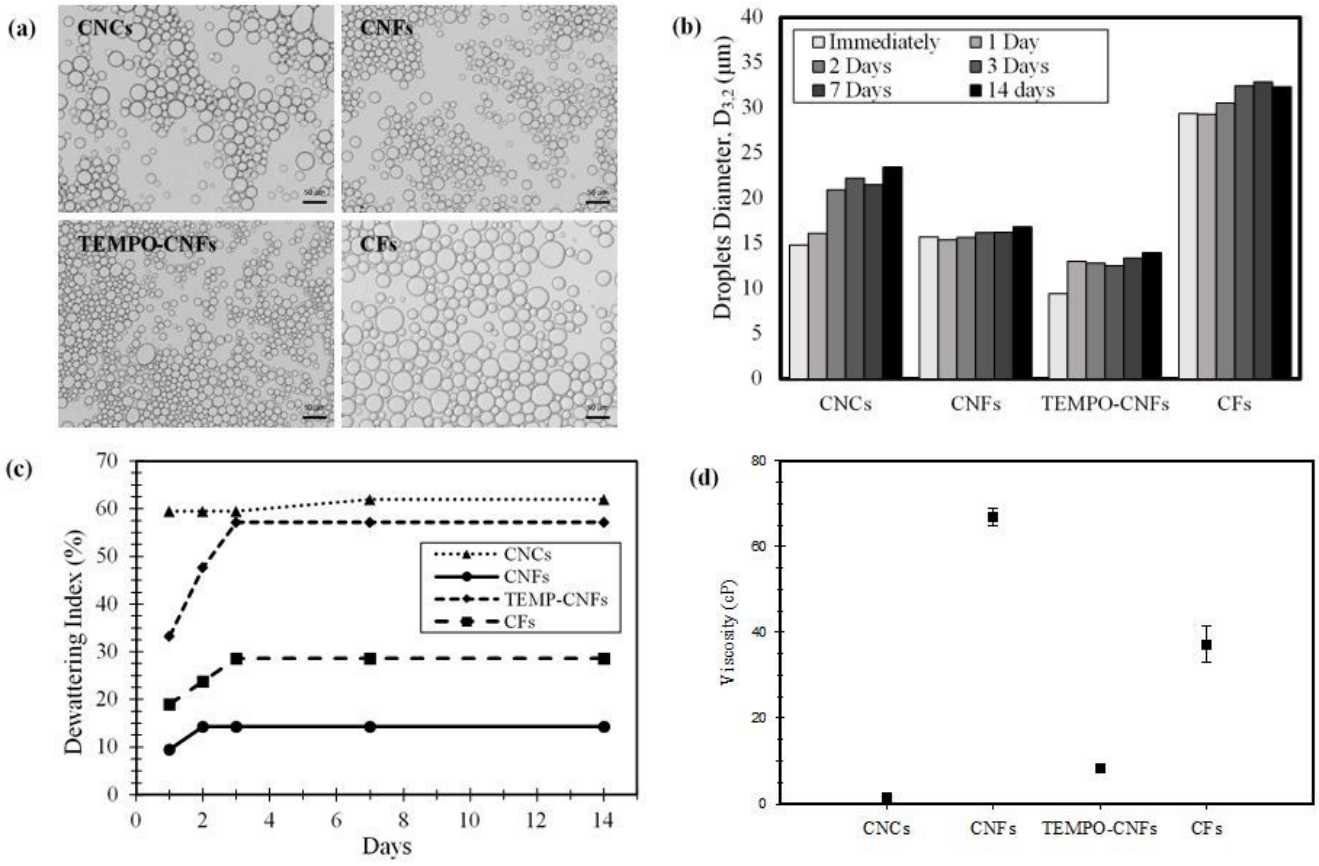

Figure 5

Comparison of the capability of different celluloses on stabilizing O/W emulsions at particle concentration of 0.25 wt% (a) microscope images of the stabilized emulsions, (b) average diameter of the droplets (D3, 2), (c) dewatering index, (d) viscosity of suspensions with 0.5 wt% concentration at a shear rate of 50 1/s.

Supplementary Files

This is a list of supplementary files associated with this preprint. Click to download.

- Supplementary.docx